

Iowa State University

From the Selected Works of Kristen P. Constant

September, 1996

Microstructure development in furfuryl resin-derived microporous glassy carbons

Kristen P. Constant, *Massachusetts Institute of Technology*

Jonq-Ren Lee, *Massachusetts Institute of Technology*

Yet-Ming Chiang, *Massachusetts Institute of Technology*



Available at: https://works.bepress.com/kristen_constant/38/

Microstructure development in furfuryl resin-derived microporous glassy carbons

Kristen Persels Constant,^{a)} Jonq-Ren Lee, and Yet-Ming Chiang

Department of Materials Science and Engineering, Massachusetts Institute of Technology, Cambridge, Massachusetts 02139

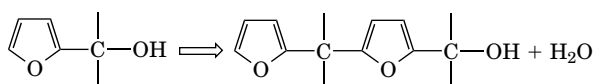
(Received 28 November 1995; accepted 28 May 1996)

The processing of microporous glassy carbon derived from furfuryl alcohol and ethylene glycol mixtures has been studied, with emphasis on understanding and controlling microstructure development. It is shown that this system exhibits a polymerization-dependent miscibility gap, and that the carbon microstructure is determined by phase separation in the liquid state. Variations in carbon microstructure with composition and thermal history can be understood in terms of the time-dependent immiscibility and resulting phase separation.

I. INTRODUCTION

Glassy carbon has been used for a number of applications, including filters, electrodes, molecular sieves, and catalyst supports, since its discovery in the early 1960's.^{1,2} More recently a microporous form of glassy carbon³ has found use as a preform for reaction forming of structural ceramics.⁴⁻⁷ In this application, the uniformity, density, pore size, and pore interconnectivity of the carbon preform play an important role in determining the rate of infiltration and reaction and the resulting microstructure. Control of the carbon microstructure is therefore crucial for control of the reaction-forming process. The liquid-based system for producing microporous carbon discussed here was first described by Hucke in 1975.³ The carbon-yielding furfuryl resin is first mixed with a pore-forming alcohol and optional inert ingredients. Thermal polymerization of the furfuryl resin, catalyzed by acid, results in a rigid solid from which the fluid pore former can be removed. The body is then pyrolyzed in inert atmosphere to form porous glassy carbon. The microstructure of the resulting body appears to be defined by a number of parameters including the ratio and specific composition of the components, as well as the thermal history of the mixture.

The mechanisms responsible for the evolution of microstructure, and the methods of controlling the microstructure, have not previously been investigated in detail. However, the polymerization of furfuryl alcohol is known to occur by the following condensation reaction⁸:



^{a)}Now at Iowa State University, Materials Science and Engineering, Ames, Iowa 50010.

Significant crosslinking occurs with a maximum of four linkage points per monomer unit. It has not been determined whether this crosslinking occurs during growth of the polymer chains or afterward. Regardless, as the polymer chains lengthen, the viscosity increases significantly, and mobility decreases.⁸ In this study, we explore the effects of various processing parameters and show that the microstructure of these glassy carbons is predominantly determined by phase separation in the liquid state, occurring concurrently with polymerization, prior to pyrolysis.

II. EXPERIMENTAL PROCEDURE

A. Composition

Although several starting materials were investigated, the most comprehensive set of experiments was performed using furfuryl alcohol monomer or furfuryl alcohol homopolymer (Quacorr® Furfuryl Alcohol and 1300 Resin, QO Chemicals, West Lafayette, IN 47906) (M.W. 98 and ~300, respectively) as the carbon precursor. Ethylene glycols of different molecular weights were used in varying proportions as the second component, and paratoluene sulfonic acid (PTSA) was used as a catalyst. The principal compositional variables were the resin-to-glycol ratio, the molecular weight of the glycol (varying from ethylene glycol to tetraethylene glycol), and the water content (Table I). We will discuss the effects of variations in composition with respect to a reference composition of 50 wt.% of a resin mixture and 50 wt.% of a glycol mixture composed of 33:67 diethylene glycol:triethylene glycol by weight, with 4 wt.% PTSA. In all experiments the resin mixture was composed of 50% homopolymer and 50% monomer by weight. From this reference composition, the effect of the solvent composition was studied by systematically varying the proportions from pure ethylene glycol, (EG)

TABLE I. Compositions investigated.

Resin/solvent ratio wt. %	Glycol composition wt. %	Water content wt. % (of resin)	No. of samples
50:50	EG:TEG 0:100–25:75	0	6
	EG:TetEG 0:100–25:75		6
	DEG:TEG 0:100–100:0		7
	DEG:TetEG 0:100–100:0		7
40:60–60:40	100% DEG	0	3
	100% TEG		5
	100% TetEG		5
45:55	DEG-TEG 83:17–17:83	0	5
55:45	DEG-TEG 33:67	0	1
45:55	100% DEG	0–2.5%	8
50:50	100% TEG	0–2.0%	5
50:50	100% TetEG	0–2.0%	5

EG–Ethylene Glycol
 DEG–Diethylene Glycol
 TEG–Triethylene Glycol
 TetEG–Tetraethylene Glycol

(the lowest molecular weight glycol), to pure tetraethylene glycol, (TetEG) (the highest molecular weight glycol studied). Several combinations and ratios of EG, diethylene glycol, (DEG), triethylene glycol, (TEG), and TetEG were studied. The solvent-to-resin ratio was also varied from 40:60 to 60:40. The effect of intentionally added water was also studied at concentrations from 0% to 2.5% by weight.

B. Thermal treatment

After the solid acid was dissolved in the ethylene glycol, the resin was added and stirred mechanically for 10 min at room temperature. The mixture was then poured into glass tube molds and placed in a drying oven at 40 °C for 4 h for low temperature annealing. The sample was then placed in a convection dryer at 70 °C for further annealing during which substantial polymerization occurs. After 2 h, the rigid body was removed from the mold and excess glycol removed by draining with absorbent paper. The samples were then held at 70 °C for an additional 22 h. The sample was pyrolyzed by slowly ramping to 700 °C in flowing nitrogen and held for 1 h. The thermal history profile is illustrated in Fig. 1.

The resulting microstructure was characterized by scanning electron microscopy. The pore size, size distribution, and skeletal density (of the carbon) were characterized using mercury porosimetry. Hot-stage optical microscopy was also used to observe immiscibility in the fluid components at lower temperature (e.g., before pyrolysis).

III. RESULTS

The reference composition produced a co-continuous network structure with pore and carbon

dimensions that were on the order of 1 μm (Fig. 2). An important observation is that the co-continuous network is fully developed after polymerization, and is not a product of the pyrolysis step. This is clearly demonstrated by the comparison of microstructures immediately after polymerization (before pyrolysis), and after pyrolysis at 700 °C, shown in Figs. 2(a) and 2(b), respectively. Except for a slight change in scale due to shrinkage upon pyrolysis, the co-continuous morphology is identical before and after pyrolysis. The bulk density of this structure is 0.91 gm/cm^3 , 59% of that of fully dense glassy carbon produced from polymerized furfuryl alcohol.¹ Mercury porosimetry results in Fig. 3 show that the average pore size is approximately 1 μm , and that the pore size distribution is narrow. The microstructural features of preforms prepared from these and of other compositions are summarized in Table II.

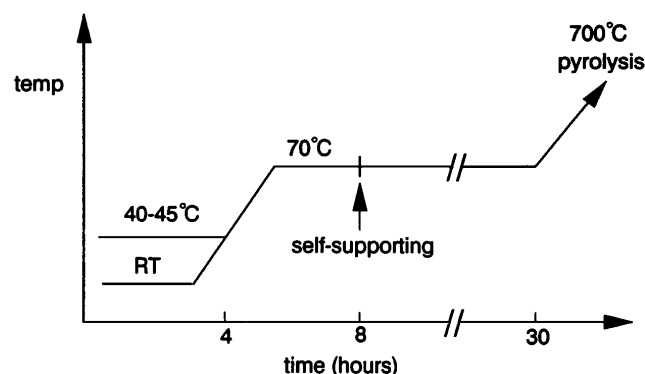


FIG. 1. Time-temperature profile for processing of microporous carbons.

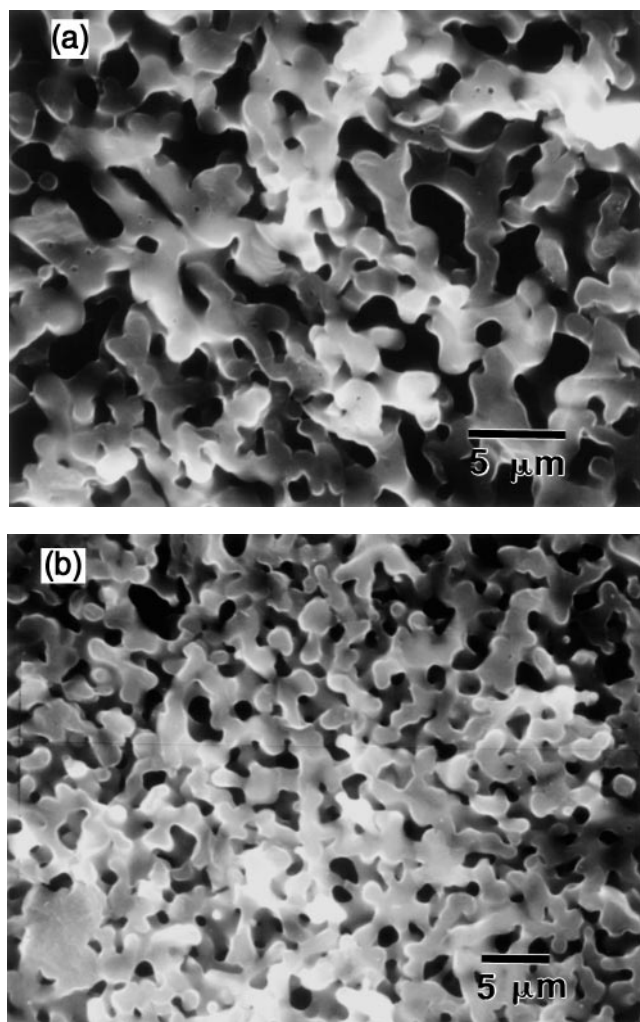


FIG. 2. Microstructure showing co-continuous phases: (a) after polymerization and before pyrolysis, in which the solid phase is polymerized furfuryl alcohol resin; and (b) after pyrolysis to glassy carbon.

A. Low temperature miscibility

Miscibility in the starting resin/glycol solutions was studied using an optical microscope equipped with a heating stage. The ratio of furfuryl resin to glycol was the same as used in preparing preforms, but the catalyst was excluded in order to inhibit polymerization during observation. We observed that at room temperature the monomer is fully miscible in all of the glycol mixtures studied. On the other hand, the homopolymer is not fully miscible at room temperature in any of the glycols at the ratios used, although a greater solubility is evident in the lower molecular weight glycols. Upon heating to 70 °C, however, all homopolymer-glycol mixtures became miscible, forming a single phase liquid. When these mixtures were cooled to room temperature, a large volume fraction of spherulites formed, confirming the immiscibility. At an intermediate temperature of 40 °C, as used in processing (Fig. 1), the homopolymer was

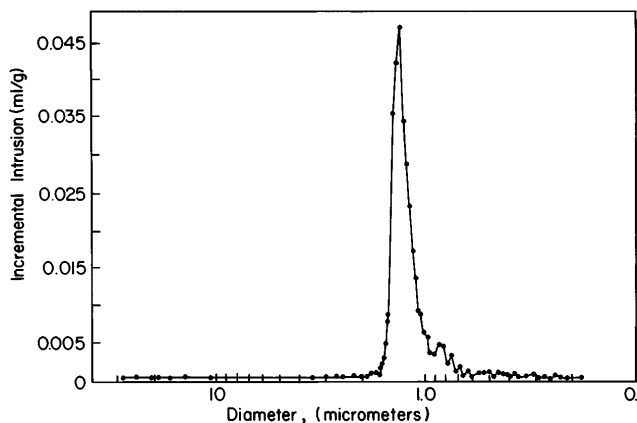


FIG. 3. Pore size distribution in microporous glassy carbon [Fig. 2(b)] showing a narrow size distribution centered near 1 μm , from mercury intrusion porosimetry.

again miscible in the glycol mixtures, but dissolution was slow. Given adequate holding time (e.g., 4 h), most of the compositions studied reached a single phase liquid.

These observations show that miscibility is a function of the molecular weights of both the furfuryl resin and the ethylene glycol, and that at the temperatures used in the early stages of the thermal cycle, a single phase liquid can be achieved given sufficient holding time. In the initial stages of processing, complete dissolution of the homopolymer is important for obtaining homogeneous microstructures. If polymerization was induced (in mixtures containing catalyst) before the homopolymer completely dissolved, large carbon particles were visible in the final microstructure. Uniform microstructures were obtained when the starting state was a single phase liquid. The results discussed later are solely from these materials.

The results also show that as polymerization proceeds, thereby increasing the average molecular weight of the furfuryl resin, an increasing degree of immiscibility with the glycol component will develop. Thus the furfuryl resin-glycol miscibility is time-dependent in the present process. This is a key result for understanding the development of microstructure.

B. Resin-to-glycol ratio

The primary effect of varying resin-to-glycol ratio is to alter the morphology and interconnectivity of the final microstructures in the pyrolyzed carbons (Fig. 4). A secondary effect on the scale of the microstructure was also observed. These correlations are listed in detail in Table II. We distinguish between co-continuous morphologies, here taken to mean those in which both phases are smoothly interconnected in three dimensions, and discrete particulate morphologies, which can nonetheless be interconnected due to packing considerations. At a resin-to-glycol volume ratio of 50:50, a co-continuous

TABLE II. Microstructural characteristics of microporous carbons as a function of composition.

Resin/glycol	Glycol composition	Pore size μm	Microstructure description
50:50	EG:TEG 0:100 10:90	<0.5	Fine, co-continuous structure
		4	Coarser, co-continuous structure, with secondary phase separation (pores) in carbon phase
		≥ 5	Still coarser co-continuous structure with secondary phase separation in pore phase (isolated carbon spheres)
	EG:TetEG 0:100 15:85 25:75	≤ 0.5	Very fine, co-continuous structure
		1–2	Co-continuous structure
		>5	Coarser co-continuous structure with secondary phase separation in both phases (isolated carbon spheres)
	DEG:TEG 0:100 33:67 67:33 100:0	<0.5	Fine, co-continuous microstructure
		1	Reference composition (see Fig. 2)
		3–4	Secondary phase separation in pore phase (isolated carbon spheres $\sim 1 \mu\text{m}$)
		>5	Secondary phase separation in pore phase (isolated carbon spheres $\sim 2 \mu\text{m}$)
	DEG:TetEG 0:100 33:67 67:33 100:0	<0.1	Very fine, co-continuous structure
		0.5	Fine, co-continuous structure
		1.5	Co-continuous, with secondary phase separation in pore phase (isolated carbon spheres)
		5	Co-continuous, with secondary phase separation in pore phase (isolated carbon spheres $\sim 2 \mu\text{m}$)
45:55	DEG:TEG 17:83 50:50 83:17	0.1	Co-continuous microstructure
		1	Co-continuous microstructure
		...	Loosely packed isolated spheres ($\sim 2 \mu\text{m}$ diameter)
55:45	DEG:TEG 33:67	5	Co-continuous, with secondary phase separation in both phases (isolated spheres $\sim 1.5 \mu\text{m}$ and pores $\sim 1.5 \mu\text{m}$)
40:60–60:40	100% DEG	...	Loosely packed isolated spheres; decreasing sphere size with increasing glycol content
	100% TEG	...	Extremely fine structure; samples cracked on pyrolysis; pore size $\sim 0.5 \mu\text{m}$
	100% TetEG	...	Extremely fine structure for all resin/glycol ratios

structure was always formed, the scale of which varied in detail with composition [Figs. 2, 4(b)]. At a ratio of 45:55, a co-continuous morphology could be achieved only for certain compositions, while in others discrete spherical carbon particulates were obtained. At 40:60 ratio (the lowest examined) the carbon always appeared as spherical particulates [Fig. 4(a)]. When the resin/glycol ratio was varied to give an excess of resin, at a ratio of 55:45 a co-continuous microstructure could still be obtained, but at higher ratios (60:40) spherical droplets of glycol formed in a matrix of resin [Fig. 4(c)]. This morphology was generally undesirable since the preforms tended to crack upon pyrolysis as the glycol volatilized from the enclosed porosity.

C. Glycol composition

The glycol composition primarily influenced the scale of the final microstructure. Examination of the results in Table II shows that for a given resin/glycol ratio, lowering the average molecular weight of the glycol mixture causes an increase in the scale of the microstructure. This trend is clearly observed for all of the resin/glycol ratios examined. The coarsest microstructure

obtained had pore dimensions exceeding $5 \mu\text{m}$ and spherical carbon dimensions of $\sim 2 \mu\text{m}$, while the finest were unresolvable by conventional SEM (e.g., less than $\sim 0.5 \mu\text{m}$). Mercury porosimetry showed average pore sizes as fine as $0.1 \mu\text{m}$ in some of these materials. As discussed later, we believe the effect of glycol molecular weight to be primarily the result of viscosity on phase separation kinetics; the viscosity at room temperature varies from 0.179 Ps-s for ethylene glycol to 0.582 Pa-s for tetraethylene glycol.

D. Secondary phase separation

Secondary phase separation is the precipitation of a phase within a phase, and can occur when a region of a phase-separated microstructure is physically isolated and develops further immiscibility. In silicate glasses, secondary and multiple phase separation is frequently observed upon cooling, and is manifested as a microstructure with several levels of increasingly finer decomposition, as illustrated by Vogel.⁹ In this study we frequently observed evidence for secondary phase separation in the form of smaller spherical pores within

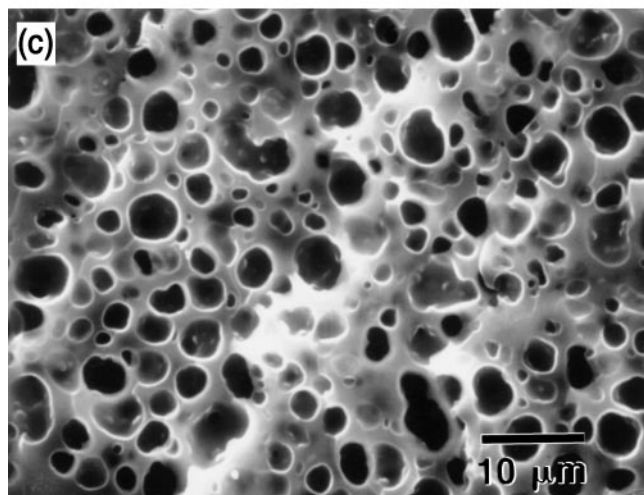
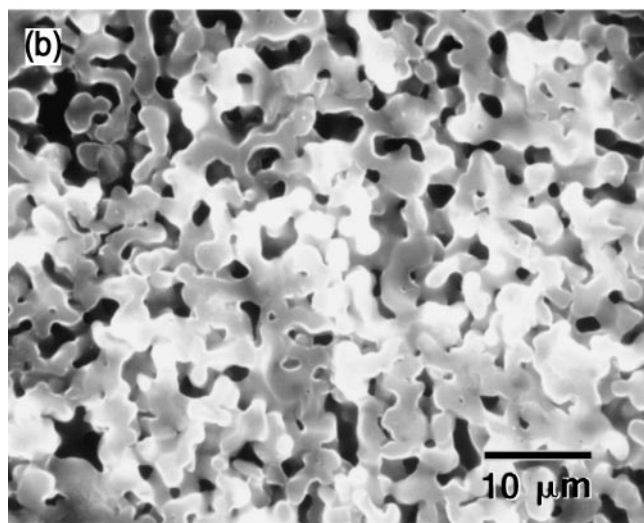
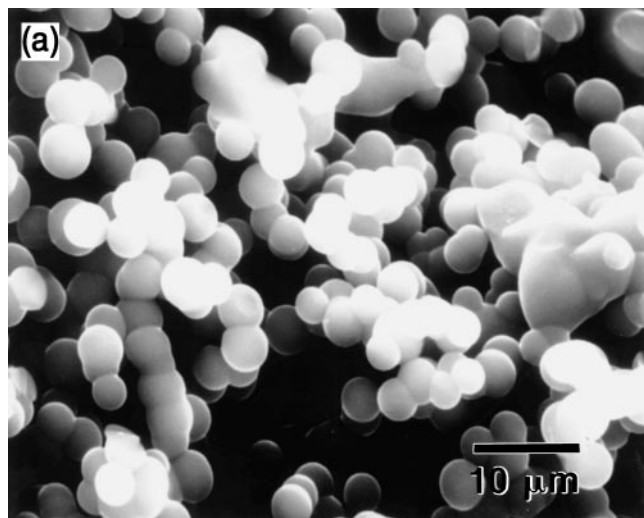


FIG. 4. Variation in morphology and connectivity of the carbon and pore phase as a function of the furfuryl resin/glycol ratio: (a) 40 : 60; (b) 50 : 50; (c) 60 : 40.

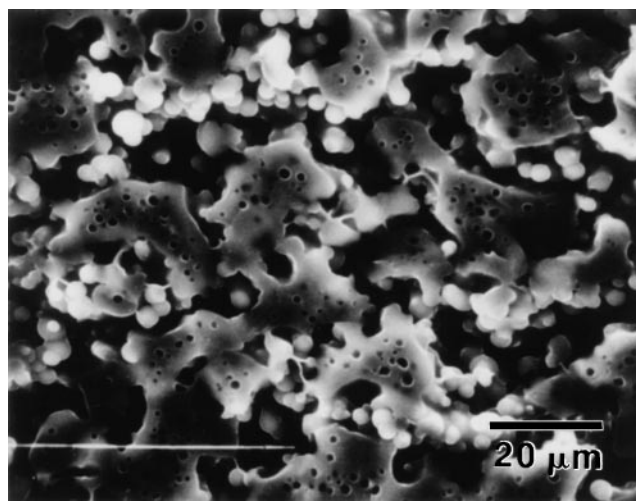


FIG. 5. Secondary phase separation within the primary phases, manifested as spherical (glycol-filled) pores within the furfuryl resin-rich phase and spherical carbon particulates within the pore phase (ethylene glycol-rich prior to pyrolysis).

the glassy carbon phase, and smaller carbon spheres within the open porosity, as illustrated in Fig. 5.

In some samples both features were simultaneously observed; in others, only one. Within either primary phase, secondary phase separation was observed only when the primary phase dimensions exceeded $\sim 2 \mu\text{m}$, as shown in Table II. A systematic correlation was also observed between secondary phase separation and composition. Secondary phase separation within the carbon phase, manifested as spherical porosity, tended to occur with the higher molecular weight glycols (TEG, TetEG) but not with DEG. This may be the result of a greater initial solubility of the higher molecular weight glycols in the resin, which then precipitates as polymerization occurs. It may also be the result of slower phase separation kinetics due to the greater viscosity, or may be a combination of both factors. Secondary phase separation within the glycol-rich (pore) phase, manifested as the appearance of small carbon spheres, could not clearly be correlated with composition, although one expects that both solubility and diffusion kinetics within this phase are composition-dependent as well.

E. Role of water

Water added directly to the resin-glycol mixture is expected to inhibit the condensation polymerization reaction, delaying the increase in viscosity of the furfuryl resin and the development of immiscibility. We observed that increasing the water content can dramatically increase the scale of the resulting microstructure. This is illustrated in Figs. 6 and 7 and Table III. The addition of 2.0% water can increase the microstructural scale from less than $1 \mu\text{m}$ to tens of micrometers. The scale of the secondary phase separation increases simultaneously

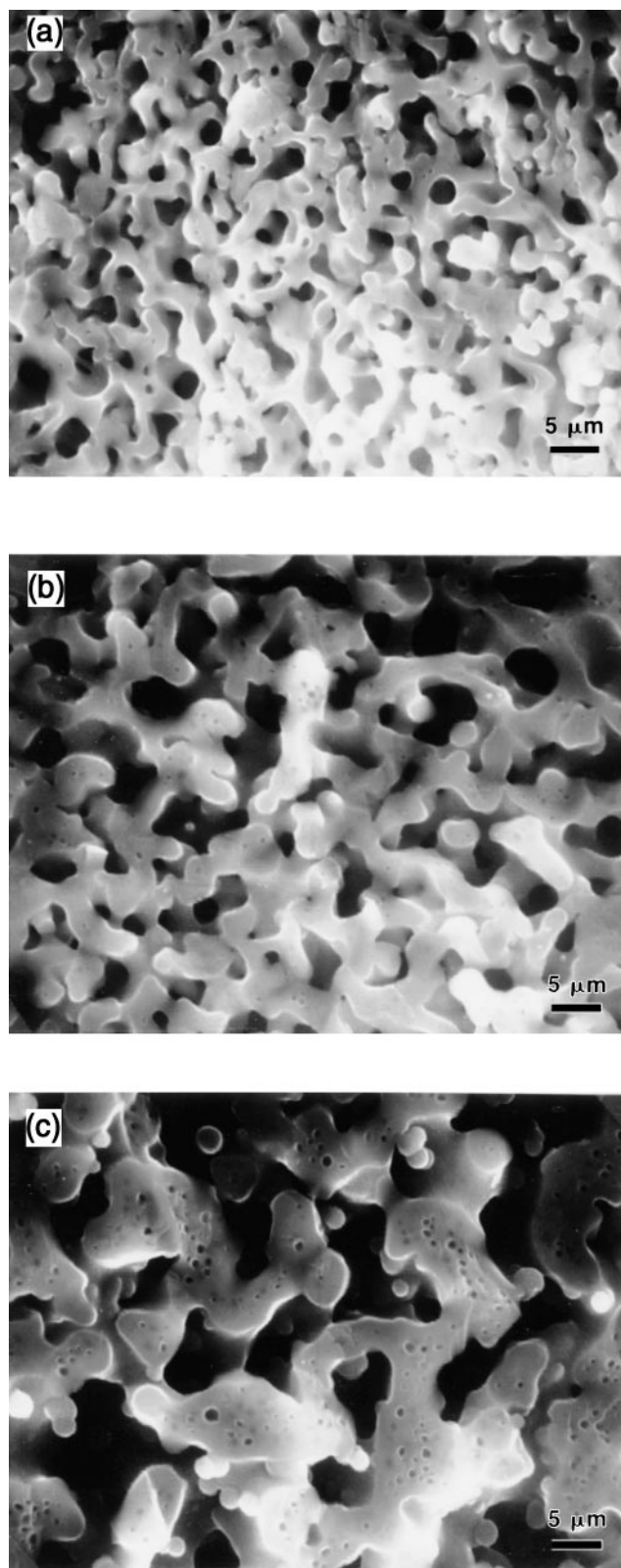


FIG. 6. Influence of water addition on the microstructure of the "reference" composition (see Table II): (a) no water; (b) 0.5 wt. % water; (c) 0.75 wt. % water. Water inhibits the condensation polymerization of furfuryl resin and results in greater coarsening during phase separation.

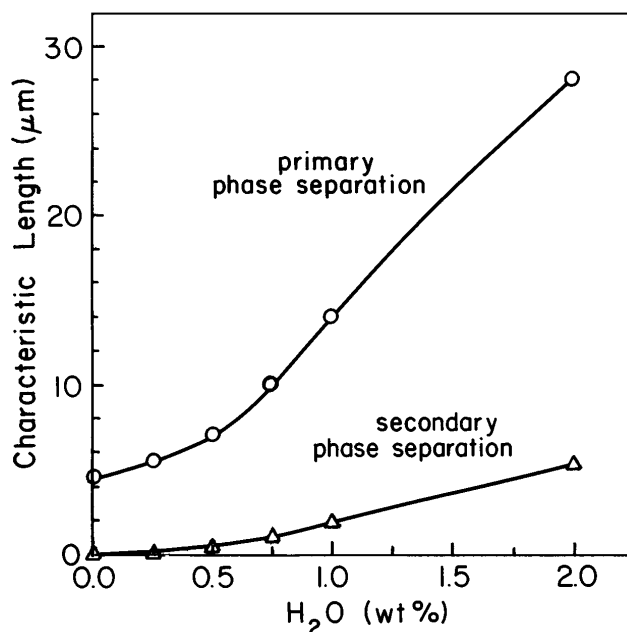


FIG. 7. Influence of water on the length scale of the carbon microstructure and the secondary phase separation, in the reference composition.

(Fig. 7). An exception was the composition prepared with TetEG alone (Table III), in which all microstructures remained below SEM-resolvable scales even with water additions. In this composition there may still be systematic variations with water content observable only at higher magnification.

Given the influence of water on polymerization, it is not surprising that the control of ambient humidity and rate of water loss by vaporization during the process (i.e., the geometry of the mold or convection from the surface) will also have an influence on the microstructure. While these effects are too complex to discuss in detail here, it is noted that the experiments presented above were conducted in a consistent manner so as to eliminate evaporative water loss rate as a variable.

F. Other compositional effects

The rate of polymerization did not vary with acid catalyst in the range of concentrations (2–8 wt. % with respect to the resin) studied. However, if the catalyst was not added, polymerization did not occur at an appreciable rate; the mixtures remained fluid indefinitely. Polymerization was also affected by the monomer-to-homopolymer ratio, proceeding much faster for high monomer content compositions. A runaway exothermic reaction followed by rapid solidification tended to occur in compositions containing only monomer. This is also why the experiments discussed here were all conducted using a resin mixture containing 50% monomer and 50% homopolymer.

TABLE III. Influence of water additions on microstructure.

Resin/glycol	Glycol composition	Water wt. %	Pore size μm	Microstructure description
45:55	100% DEG	0–2.5	...	Loosely packed isolated spheres, increasing in diameter with water content from 2 μm at 0% water to 5 μm at 2.5% water
50:50	100% TEG	0	<0.5	Co-continuous microstructures, in which carbon scale and pore size increase with increasing water content
		1.0	1	
		2.0	3.5	
50:50	100% TetEG	0–2.0	...	All very fine structure, below SEM resolution

IV. DISCUSSION

All of the above results can be reconciled with a model in which polymerization-dependent phase-separation in the liquid state determines the microstructure. It is clear that the carbon microstructure forms as a result of phase separation in the liquid state, rather than as a result of the pyrolysis process. In order to obtain samples that are microstructurally uniform after pyrolysis, we observe that it is necessary to begin with a single-phase liquid. Immiscibility is observed to develop concurrently with polymerization, with only two liquid phases being evident: a furfuryl resin-rich phase and a glycol-rich phase. The former becomes the glassy carbon network, while the latter results in porosity. We may therefore view the microstructure development process as polymerization-dependent immiscibility in a pseudobinary system, illustrated in Fig. 8, the distinction with inorganic systems being that the “equilibrium” immiscibility is time-dependent. As the single-phase liquid is held at constant temperature (e.g., 70 °C), the immiscibility region grows to encompass the experimental composition. The connectivity of the two phases is predominantly determined by the relative

volume fractions of the two phases, while the scale of the microstructure is determined by phase-separation kinetics influenced by the relative molecular weights of the endmembers, the water content, and the specific thermal history.

Although we have not examined the specific compositions of the two liquid phases, the general shape of the miscibility gap can be deduced from the composition-dependence of microstructure, tabulated in Table II. The appearance of co-continuous phases for 50:50 mixtures (by volume) of the furfuryl resin and glycol indicates that the miscibility gap is, first of all, relatively symmetric. In detail, variations in which the secondary phase separation appears (i.e., as discrete pores in the carbon or as carbon spheres in the porosity) are seen with changing glycol composition. These effects are relatively minor and may be attributable to phase separation kinetics as well as any shift in the immiscibility field. From results for other resin/glycol ratios, however, it does appear that the glycol component has an influence on the asymmetry and/or position of the miscibility gap. Considering the results for the 45:55 resin/glycol mixture, we see that it evolves from co-continuous microstructures to discrete carbon spheres as the DEG fraction in the glycol increases. This suggests a steeper phase boundary on the glycol-rich side of the gap and a more gradual slope on the resin-rich side at the lower glycol molecular weight (i.e., the critical concentration is shifted toward the glycol-rich end). The fact that the sample of 55:45 ratio has a co-continuous structure is consistent with such an asymmetry. In compositions where only DEG is used as the glycol component, discrete carbon spheres are seen over the entire range of resin/glycol ratios from 40:60 to 60:40, indicating that the gap is either asymmetric as discussed above or that the gap is displaced toward the glycol-rich end. However, when the average molecular weight of the glycol is increased by adding TEG or TetEG, co-continuous structures are again obtained, indicating a largely symmetric gap.

While this simplified view is consistent with the experimental results, in detail, the shape of the gap may also be polymerization-dependent, since polymerization

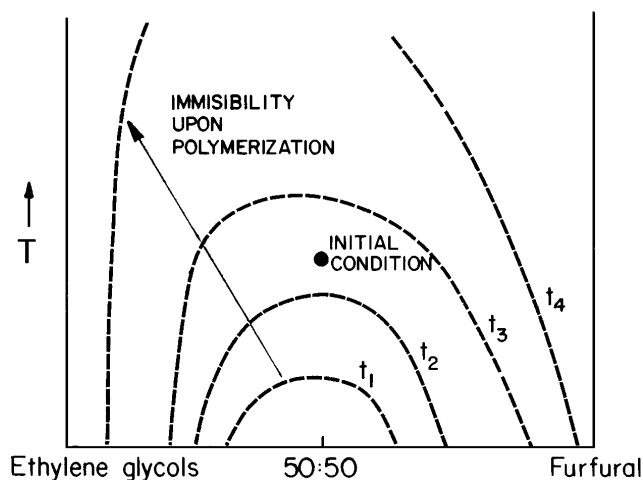


FIG. 8. Polymerization-dependent immiscibility. An initial single-phase liquid held at a constant temperature undergoes phase separation as the immiscibility field grows to encompass it.

occurs preferentially in the furfuryl resin-rich phase. As discussed recently by Nose,¹⁰ polymer/solvent solutions tend to exhibit asymmetric phase diagrams, with the critical concentration, ϕ_c , becoming increasingly polymer-rich in reciprocal proportion to the square root of the degree of polymerization, P : $\phi_c \sim P^{-1/2}$. It is also possible that the connectivity of the phases evolves in time, particularly for mixtures near the boundary between clearly co-continuous and clearly discrete morphologies. As with phase-separated microstructures in inorganic systems,¹¹ we expect that phase separation within the spinodal will yield an initially co-continuous microstructure, whereas separation outside the spinodal yields initially discrete phases by nucleation and growth. However, what subsequently transpires is less clear, with Haller¹² having argued that an interconnected phase morphology can appear via the coalescence of initially separated particulates, while Mazurin and Porai-Koshits¹³ argued that an interconnected structure can ripen into an isolated structure but the reverse cannot occur.

The appearance of co-continuous microstructures in many of the samples examined here certainly suggests a spinodal phase separation mechanism. Spinodal decomposition is well-known in polymers,^{10,14–18} and reaction-induced decomposition¹⁹ as well as the freezing-in of a decomposed state by crosslinking¹⁵ have been previously observed. Unlike inorganic systems, in which submicron length scales are generally observed in spinodally decomposed microstructures, the concentration fluctuations and cluster size are large enough in macromolecular systems that micrometer (and larger) scale spinodal phase separation is observed.^{10,20} However, most studies have been concerned with systems in which both endmembers are extensively polymerized, rather than polymer/solvent mixtures like that studied here. While the mechanism of phase separation in the present samples (particularly the co-continuous structures) is highly likely to be spinodal decomposition, this cannot be conclusively determined without detailed information on the kinetics of decomposition, or direct evidence for diffuse interfaces associated with the spinodal mechanism as seen in some glasses.²¹

V. CONCLUSIONS

The evolution of microstructure in porous glassy carbons derived from mixtures of furfuryl resin and ethylene glycols has been systematically investigated as a function of composition and processing variables. It is shown that the microstructure of the final, pyrolyzed carbons are determined by phase separation in the liquid state. Starting with a single-phase solution of furfuryl resin and glycol, polymerization of the furfuryl resin component causes a time-dependent liquid-liquid immiscibility to develop between a furfuryl resin-rich phase which is ultimately pyrolyzed to glassy carbon, and a glycol-

rich phase which becomes porosity. The miscibility gap is largely symmetric, although asymmetry appears to be introduced when the glycol molecular weight is decreased. By controlling the molecular weights of the furfuryl resin and ethylene glycol components, the water content, and thermal history, a broad range of microstructures including co-continuous phases, discrete spheres of either phase, and secondary phase separation within the primary phases can be obtained, at microstructural scales ranging from $<0.1 \mu\text{m}$ to greater than $5 \mu\text{m}$.

ACKNOWLEDGMENTS

This research was supported by the Office of Naval Research under Grant No. N00014-94-1-0790, Steven G. Fishman, Program Officer. The authors thank Leszek Hozer and Matthew Galla for experimental support, and Donald R. Behrendt for assistance in the early stages of this work.

REFERENCES

1. E. Fitzer, W. Schaeffer, and S. Yamada, *Carbon* **7**, 643–648 (1969).
2. H. Eckert, Y. A. Levendis, and R. C. Flagan, *J. Phys. Chem.* **92**, 5011–5019 (1988).
3. E. E. Huckle, "Method of producing carbonaceous bodies and the products thereof," U.S. Pat. No. 3,859,421, Jan. 7, 1975.
4. Y.-M. Chiang, R. P. Messner, C. D. Terwilliger, and D. R. Behrendt, *Mater. Sci. Eng.* **A144**, 63 (1991).
5. L. Hozer, J.-R. Lee, and Y.-M. Chiang, *Mater. Sci. Eng.* **A195**, 131–143 (1995).
6. L. Hozer, J.-R. Lee, and Y.-M. Chiang, in *Advanced Synthesis and Processing of Composites and Advanced Ceramics*, edited by K. V. Logan, Z. A. Munir, and R. M. Spriggs (Ceram. Trans. **56**, The American Ceramic Society, Westerville, OH, 1995), p. 158.
7. L. Hozer and Y.-M. Chiang, unpublished research.
8. E. Fitzer and W. Schafer, *Carbon* **8**, 353–364 (1970).
9. W. Vogel, *Chemistry of Glass*, 2nd ed. (Springer-Verlag, Berlin, 1994).
10. T. Nose, *Phase Trans.* **8**, 245–260 (1987).
11. J. W. Cahn and R. J. Charles, *Phys. Chem. Glasses* **6**, 181 (1965).
12. W. Haller, *J. Chem. Phys.* **42**, 686 (1965).
13. O. V. Mazurin and E. A. Porai-Koshits, in *Phase Separation in Glass*, edited by O. V. Mazurin and E. A. Porai-Koshits (North-Holland, 1984), p. 166.
14. K. Binder, *J. Phys. Chem. Solids* **79**, 6387–6409 (1983).
15. T. Hashimoto, M. Takenaka, and H. Jinnai, *Polymer Commun.* **30**, 177–179 (1989).
16. P. Pincus, *J. Chem. Phys.* **74**, 1996–2000 (1981).
17. T. Hashimoto, M. Itakura, and H. Hasegawa, *J. Chem. Phys.* **85**, 6118–6128 (1986).
18. M. Takenaka, T. Izumitani, and T. Hashimoto, *Macromolecules* **20**, 2257–2264 (1987).
19. K. Nakanishi and N. Soga, *J. Am. Ceram. Soc.* **74**, 2518–2530 (1991).
20. K. Yamanaka, Y. Takagi, and T. Inoue, *Polymer* **60**, 1839–1844 (1989).
21. Y.-M. Chiang and W. D. Kingery, *J. Am. Ceram. Soc.* **66** (9), C171–172 (1983).